

# Inhibition of miR-449a Promotes Cartilage Regeneration and Prevents Progression of Osteoarthritis in *In Vivo* Rat Models

Dawoon Baek,<sup>1,2</sup> Kyoung-Mi Lee,<sup>1,3</sup> Ki Won Park,<sup>1,2</sup> Jae Wan Suh,<sup>5</sup> Seong Mi Choi,<sup>1,2</sup> Kwang Hwan Park,<sup>1</sup> Jin Woo Lee,<sup>1,2,3</sup> and Sung-Hwan Kim<sup>4</sup>

<sup>1</sup>Department of Orthopaedic Surgery, Yonsei University College of Medicine, 50-1 Yonsei-ro, Seodaemun-gu, Seoul 03722, South Korea; <sup>2</sup>Brain Korea 21 PLUS Project for Medical Sciences, Yonsei University College of Medicine, 50-1 Yonsei-ro, Seodaemun-gu, Seoul 03722, South Korea; <sup>3</sup>Severance Biomedical Science Institute, Yonsei University College of Medicine, 50-1 Yonsei-ro, Seodaemun-gu, Seoul 03722, South Korea; <sup>4</sup>Department of Orthopaedic Surgery, Yonsei University College of Medicine, Gangnam Severance Hospital, 211 Eonju-ro, Gangnam-gu, Seoul 06273, South Korea; <sup>5</sup>Department of Orthopaedic Surgery, Dankook University Hospital, Dankook University College of Medicine, 201 Manghyang-ro, Dongnam-gu, Cheonan 31116, South Korea

**Traumatic and degenerative lesions of articular cartilage usually progress to osteoarthritis (OA), a leading cause of disability in humans. MicroRNAs (miRNAs) can regulate the differentiation of human bone marrow-derived mesenchymal stem cells (hBMSCs) and play important roles in the expression of genes related to OA. However, their functional roles in OA remain poorly understood. Here, we have examined miR-449a, which targets sirtuin 1 (SIRT1) and lymphoid enhancer-binding factor-1 (LEF-1), and observed its effects on damaged cartilage. The levels of chondrogenic markers and miR-449a target genes increased during chondrogenesis in anti-miR-449a-transfected hBMSCs. A locked nucleic acid (LNA)-anti-miR-449a increased cartilage regeneration and expression of type II collagen and aggrecan on the regenerated cartilage surface in acute defect and OA models. Furthermore, intra-articular injection of LNA-anti-miR-449a prevented disease progression in the OA model. Our study indicates that miR-449a may be a novel potential therapeutic target for age-related joint diseases like OA.**

## INTRODUCTION

Traumatic and degenerative lesions of articular cartilage usually progress to osteoarthritis (OA), which is the most prevalent joint disease and a leading cause of disability. In particular, cartilage disease or injury involving damage to the articular cartilage is a serious problem due to limitations in self-repair capacity.<sup>1</sup> Therefore, various treatments have been developed to prevent cartilage degeneration and restore injured cartilage, such as microfracture, stem cell therapy, and implantation of autologous chondrocytes or bone marrow concentrates.<sup>2–4</sup> Human bone marrow-derived mesenchymal stem cells (hBMSCs) have self-renewal capacity and are multipotent, with the capacity to differentiate into chondrocytes.<sup>5,6</sup> Therefore, stem cell therapy using hBMSCs is a good option for the regeneration of damaged cartilage. Recent studies have reported that a three-dimensional scaffold that includes

hBMSCs can replace damaged tissue, leading to cartilage restoration, and when combined with cartilage-related cytokines can secrete autologous cells, enhancing the repair of damaged cartilage.<sup>7–9</sup> Additionally, intra-articular injection of hBMSCs can stimulate anti-inflammatory genes and inhibit the expression of catabolic genes such as matrix metalloproteinases (MMPs).<sup>10</sup> However, long-term expansion of hBMSCs *in vitro* has many limitations, such as loss of stemness and differentiation capacity. Due to this, various cell-based techniques have been attempted, using diverse cell sources such as induced pluripotent stem cells (iPSCs) and gene therapy strategies with chondrogenesis-related genes.<sup>11–13</sup> However, these techniques have not yet been completely established, and these challenges remain unsolved *in vivo*. Limitations in hBMSC transplantation also remain, including inefficient delivery, safety issues, difficulties in producing tissue of normal morphology, and a limited supply of healthy articular cartilage because of surgical removal.<sup>14–16</sup> Additionally, there are few *in vivo* studies examining the prevention of OA progression using stem cells.

MicroRNAs (miRNAs) are small non-coding RNAs that regulate gene expression through post-transcriptional or post-translational regulation in various biological processes and diseases.<sup>17,18</sup> The miRNAs have many benefits that have mature sequences as short and completely conserved targeting multiple vertebrate species.<sup>19</sup> Therefore, gene modulation therapy using miRNAs has emerged

Received 11 January 2018; accepted 23 September 2018;  
<https://doi.org/10.1016/j.omtn.2018.09.015>.

**Correspondence:** Jin Woo Lee, Department of Orthopaedic Surgery, Yonsei University College of Medicine, 50-1 Yonsei-ro, Seodaemun-gu, Seoul 03722, South Korea.

**E-mail:** [ljwos@yuhs.ac](mailto:ljwos@yuhs.ac)

**Correspondence:** Sung-Hwan Kim, Department of Orthopaedic Surgery, Yonsei University College of Medicine, Gangnam Severance Hospital, 211 Eonju-ro, Gangnam-gu, Seoul 06273, South Korea.

**E-mail:** [orthohwan@gmail.com](mailto:orthohwan@gmail.com)



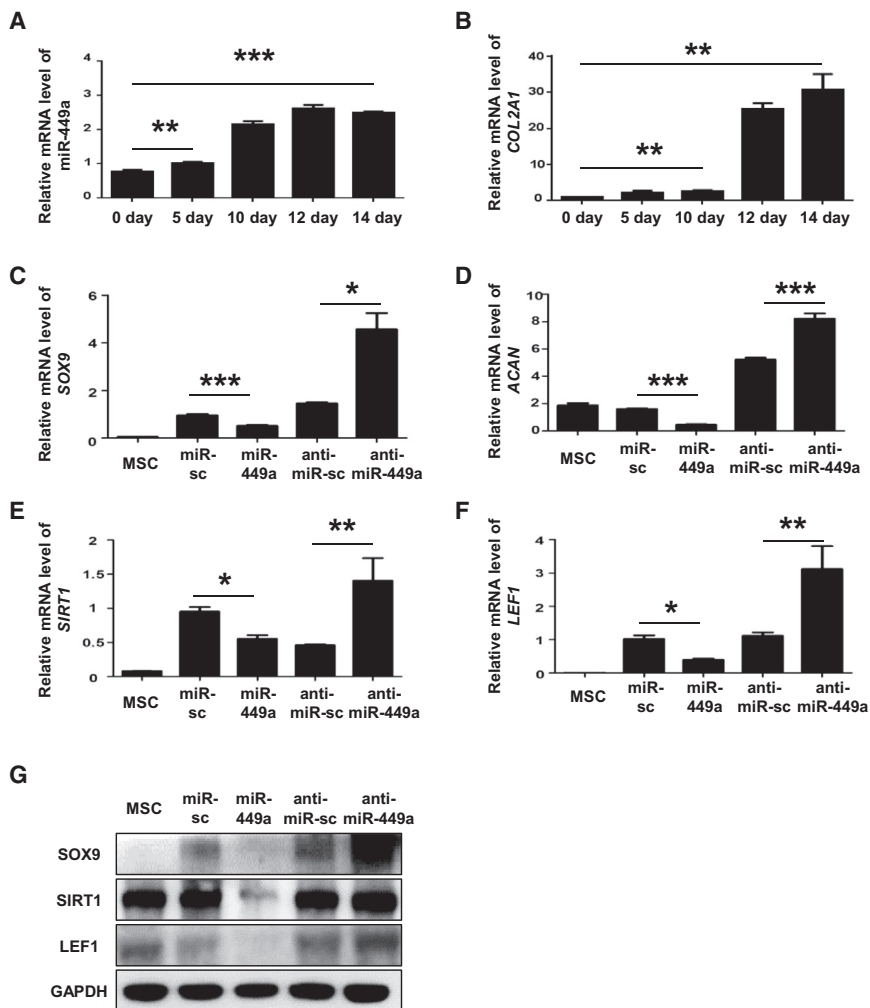


**Figure 1. Effect of miR-449a on the *In Vitro* Chondrogenic Differentiation of hBMSCs**

(A) Relative miR-449a expression during the chondrogenic differentiation of hBMSCs mass culture as determined by real-time qPCR. U6 was used for normalization. (B) Relative mRNA level of chondrogenic marker gene COL2A1 during chondrogenic differentiation of hBMSCs mass culture as determined by real-time qPCR. ACTB was used for normalization. (C–F) Relative mRNA levels of chondrogenic marker genes such as SOX9 (C), ACAN (D), and the miR-449a target genes such as SIRT1 (E) and LEF1 (F) during 5 days of chondrogenic differentiation. ACTB was used for normalization. (G) The protein levels of chondrogenic markers and miR-449a target genes during 10 days of chondrogenic differentiation. GAPDH was used as a loading control. Data are defined as mean  $\pm$  SD. p values were calculated compared with controls. \*p < 0.05; \*\*p < 0.01; \*\*\*p < 0.001 (n = 3 independent experiments).

of miRNAs as gene modulators during cartilage regeneration and OA prevention remain largely unknown.

Our group has previously demonstrated that miR-449a regulates hBMSC chondrogenesis by targeting lymphoid enhancer-binding factor 1 (LEF1).<sup>33</sup> We also revealed that miR-449a regulates expression of sirtuin 1 (SIRT1) during IL-1 $\beta$ -induced cartilage destruction, which promotes OA.<sup>34</sup> Another group reported that SIRT1 has an anabolic effect in chondrocytes and promotes the chondrogenic differentiation of hBMSCs.<sup>35</sup> Taken together, these reports indicate that miR-449a regulates the chondro-

genesis of hBMSCs and may be a useful regulator and therapeutic agent for the treatment of damaged cartilage.

as a potential therapeutic candidate against a variety of diseases.<sup>20–22</sup> Gene therapy strategies based on miRNAs have been applied to cancers both experimentally and clinically.<sup>23,24</sup> Several studies have reported that certain miRNAs are aberrantly expressed in patients with OA, indicating that miRNAs play an important role in cartilage development.<sup>25,26</sup> Recent *in vitro* studies have revealed that inhibition of miR-138-5p promotes interleukin-1 $\beta$  (IL-1 $\beta$ )-induced cartilage destruction in human chondrocytes by targeting FOXC1,<sup>27</sup> whereas miR-92a-3p regulates cartilage development and homeostasis in hBMSCs by targeting histone deacetylase 2.<sup>28</sup> miR-140-5p inhibits mediators of inflammation and promotes chondrogenesis in IL-1 $\beta$ -induced human chondrocytes, and plays roles in both cartilage development and homeostasis in miR-140-deficient mice and cartilage-specific miR-140 transgenic mice.<sup>29,30</sup> Recent *in vivo* studies have revealed that inhibition of miR-221 in hBMSCs promotes cartilage regeneration.<sup>31</sup> Another group revealed that intra-articular injection of antago-miR-483-5p blocks OA by targeting the cartilage matrix protein matrilin 3 and tissue inhibitor of metalloproteinase 2.<sup>32</sup> However, the roles

of miRNAs as gene modulators during cartilage regeneration and OA prevention remain largely unknown.

To examine *in vivo* miR-449a function, we utilized a locked nucleic acid (LNA) to stably deliver the miRNA and enhance its function. The LNA is a modified RNA nucleotide with an extra bridge linking the 2' oxygen and 4' carbon, which confers improved stability against endonucleases and exonucleases *in vivo* and effective coherence with the complementary strand.<sup>36</sup> LNA-modified miRNAs have been developed for potential applications in tumor diagnosis and treatment.<sup>37–41</sup> However, there are few studies on cartilage regeneration using LNA-modified miRNA-based gene therapies.<sup>34</sup>

In this study, we have investigated the function of miR-449a in the regulation of hBMSC chondrogenic differentiation during cartilage regeneration using an LNA-modified miRNA as a delivery system in rat acute defect and OA models. We demonstrate that miR-449a enhances cartilage regeneration in an acute defect model and prevents cartilage degeneration in an OA model by targeting LEF1 and SIRT1.

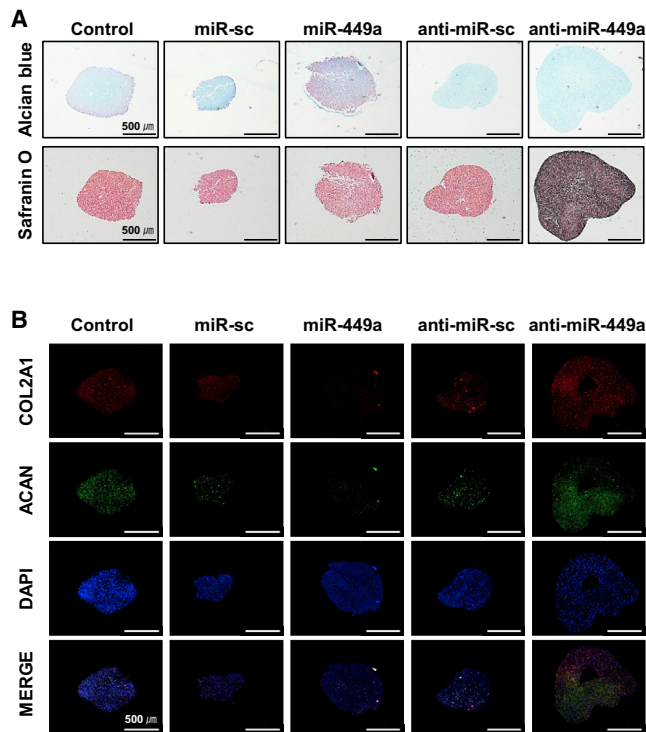


**Figure 2. miR-449a Inhibits hBMSC Chondrogenic Differentiation**

(A) Histological analysis using Alcian blue and safranin O staining during chondrogenic hBMSC micromass cultures at day 10. (B) IHC analysis of COL2A1 (phycoerythrin [PE]; red fluorescence) and ACAN (fluorescein isothiocyanate [FITC]; green fluorescence) with DAPI counterstaining 10 days after induction of chondrogenic differentiation. As a control, hBMSCs treated with TGF- $\beta$ 3 were used. Scale bars, 500  $\mu$ m (original magnification  $\times$ 4). The data were confirmed in cells from three independent donors, and representative data are shown.

Collectively, these results indicate that anti-miR-449a is a promising and novel therapeutic target for OA and general cartilage damage.

## RESULTS

### Effect of miR-449a on hBMSC Chondrogenesis

To investigate the effects of miR-449a, we observed the expression of miR-449a by miR-specific real-time qPCR at various time points during chondrogenic differentiation of hBMSCs micromass culture. The results showed that the miR-449a expression was continuously expressed and remained upregulated after induction of chondrogenesis differentiation (Figure 1A). Additionally, the expression levels of chondrogenic marker type II collagen (COL2A1) were also upregulated (Figure 1B). Next, we analyzed the mRNA levels of chondrogenic differentiation marker genes and miR-449a target genes, such as SRY-related high mobility group-box gene 9 (SOX9), aggrecan (ACAN), SIRT1, and LEF1 by real-time qPCR. The expression levels of chondrogenic differentiation marker genes were significantly decreased in miR-449a-transfected hBMSCs compared with miR-sc (control)-transfected hBMSCs. Conversely, the expression of these genes was significantly increased in anti-miR-449a-transfected hBMSCs compared

with anti-miR-sc-transfected hBMSCs (Figures 1C–1F). Furthermore, the expression levels of the miRNA-449a target genes SIRT1 and LEF1 were consistently and significantly decreased in miR-449a-transfected hBMSCs, and significantly increased in anti-miR-449a-transfected hBMSCs (Figures 1C–1F). The protein levels showed consistent trends (Figure 1G).

Finally, we confirmed the effects of miR-449a on chondrogenesis by histological analysis using Alcian blue and safranin O staining and immunohistochemistry (IHC). With Alcian blue, anti-miR-449a-transfected hBMSCs were the most positively stained (Figure 2A). With safranin O staining, the synthesis of proteoglycans was mostly increased in anti-miR-449a-transfected hBMSCs (Figure 2A). Moreover, the mass was larger in anti-miR-449a-transfected hBMSCs than in anti-miR-sc-transfected and control hBMSCs (Figure 2A). By IHC analysis, COL2A1 and ACAN expression levels were decreased in miR-449a-transfected hBMSCs (Figure 2B). However, anti-miR-449a-transfected hBMSCs displayed increased COL2A1 and ACAN expression (Figure 2B). Taken together, these results indicate that miR-449a negatively regulates the chondrogenic differentiation of hBMSCs.

### Establishment of Optimal LNA-Anti-miR-449a Concentration

To determine the effects of miR-449a on hBMSC chondrogenic differentiation during cartilage regeneration, we used LNA-anti-miR-449a, both as a delivery system and to improve the efficiency of miR-449a functional inhibition. We synthesized LNA-anti-miR-449a, with antisense oligonucleotides complementary to miR-449a (Figure 3A), and first investigated whether the synthesized LNA was cytotoxic in hBMSCs by 3-[4, 5-dimethylthiazol-2-yl]-2, 5 diphenyl tetrazolium bromide (MTT) assay. LNA-anti-miR-sc and LNA-anti-miR-449a had no effect on cell viability at all tested concentrations (Figure 3B). To establish the optimal concentration of LNA-anti-miR-449a in terms of improved target gene expression and inhibition of miR-449a expression, we treated hBMSCs with LNA-anti-miR-scramble control (LNA-anti-miR-sc) or LNA-anti-miR-449a in a dose-dependent manner and analyzed miRNA expression levels using miR-specific real-time qPCR. When hBMSCs were treated with 10–500 nM LNA-anti-miR-449a, miR-449a expression was inhibited by 50–100 nM LNA-anti-miR-449a, compared with hBMSCs treated with LNA-anti-miR-sc (Figure 3C). Next, we examined the expression of miR-449a target genes such as LEF1 and SIRT1. When hBMSCs were treated with LNA-anti-miR-449a, the mRNA expression increased in a dose-dependent manner (Figure 3D), and protein expression was enhanced at concentrations  $\geq$  50 nM (Figure 3E). For these reasons, we determined that the optimal LNA-anti-miR-449a concentration for *in vivo* treatment was 100 nM.

### LNA-Anti-miR-449a Promotes Cartilage Regeneration in an Acute Defect Model

To examine whether LNA-anti-miR-449a affected cartilage regeneration in an acute defect model, we created osteochondral defects in rats, and the defect sites were either left untreated or filled with

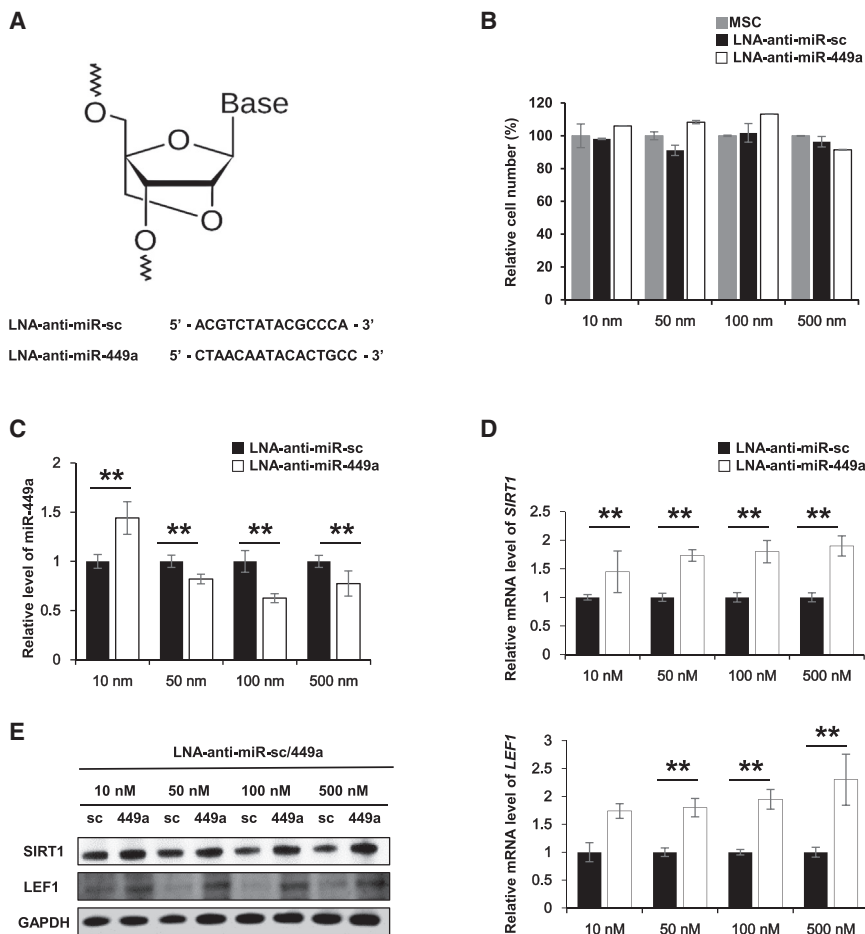


**Figure 3. Synthesis of LNA-Anti-miRs and Concentration Optimization**

(A) The structure of the LNA oligonucleotides and the sequences of the LNA-modified-anti-miR-scramble control (LNA-anti-miR-sc) and LNA-modified-anti-miR-449a (LNA-anti-miR-449a). (B) A cytotoxicity assay was performed to detect the loss of viability. (C) After treatment of hBMSCs with various concentrations of LNA-anti-miR-sc or LNA-anti-miR-449a, relative miR-449a levels were measured by miR-specific qPCR. U6 was used for normalization. (D) The mRNA levels of the miR-449a target genes *SIRT1* and *LEF1* in hBMSCs after treatment with various concentrations of LNA-anti-miR-sc or LNA-anti-miR-449a. (E) The protein levels of the miR-449a target genes *SIRT1* and *LEF1* in hBMSCs after treatment with various concentrations of LNA-anti-miR-sc or LNA-anti-miR-449a. Data are defined as mean  $\pm$  SD. \*\* $p < 0.01$  ( $n = 3$  independent experiments).

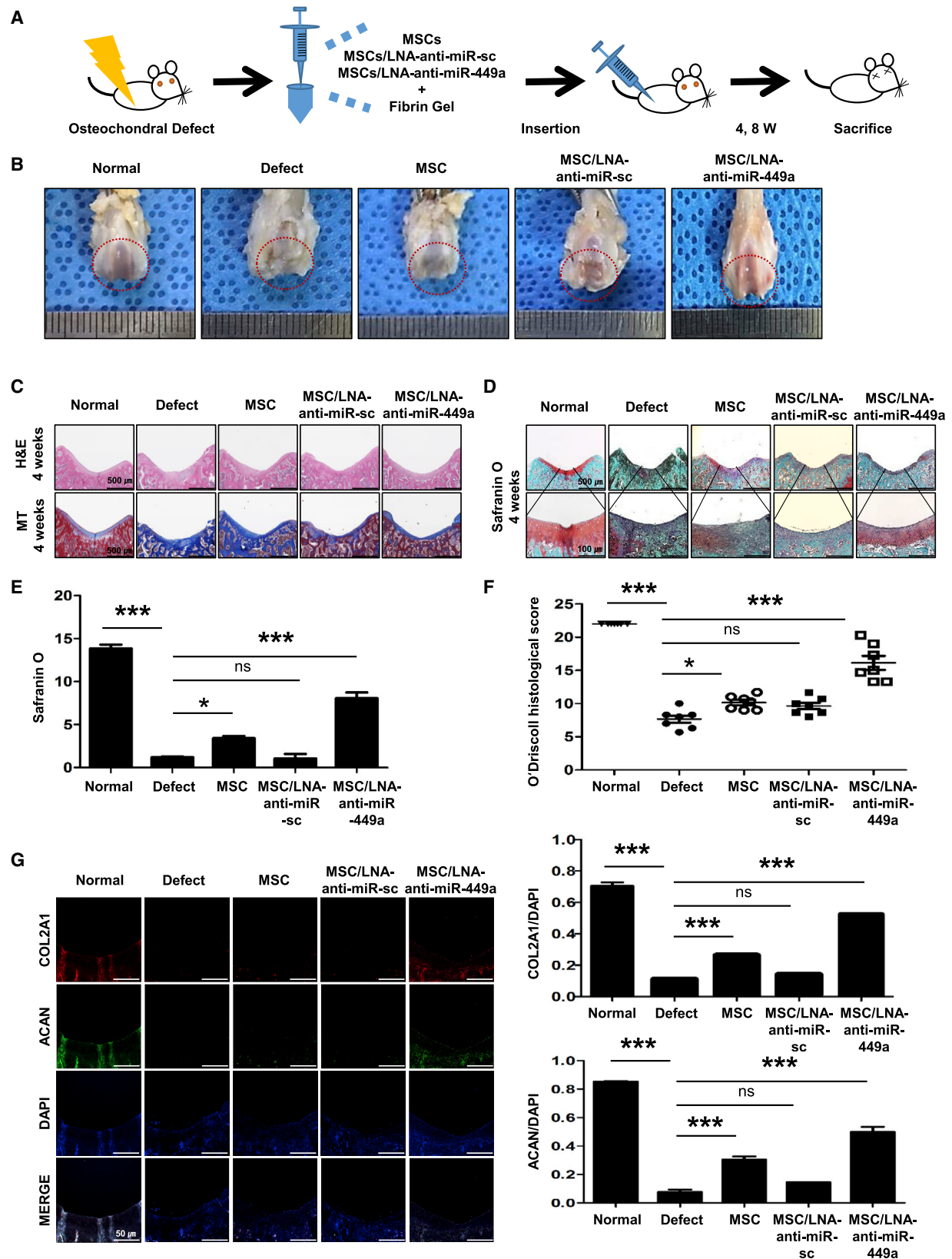
hBMSCs, hBMSCs with LNA-anti-miR-sc, or hBMSCs with LNA-anti-miR-449a (Figure 4A). Histological analysis of regenerated articular cartilage was performed 4 and 8 weeks after surgery. After 4 weeks, the regenerated cartilage in the hBMSCs with LNA-anti-miR-449a group was smooth and resembled normal cartilage tissue (Figure 4B). However, the hBMSCs and hBMSCs with LNA-anti-miR-sc groups showed comparatively insufficient cartilage regeneration. Histological features were examined by H&E and Masson's trichrome (MT) staining, and well-differentiated chondrocytes resembling those of normal cartilage were observed in the hBMSCs with LNA-anti-miR-449a group (Figure 4C). However, the other groups showed incompletely differentiated chondrocytes and severe disruption of normal cartilage surface. There was increased safranin O staining throughout the matrix, with abundant glycosaminoglycans (GAGs) and intact surface integrity in the hBMSCs with LNA-anti-miR-449a group (Figures 4D and 4E), whereas the other groups showed reduced safranin O staining. We evaluated the histological findings using a modified O'Driscoll score system (Figure 4F). The hBMSCs with LNA-anti-miR-449a group showed significantly higher scores ( $16.13 \pm 2.77$ ;  $p = 0.0001$ ; Figure 4F) than the defect ( $7.65 \pm 1.46$ ), hBMSCs

the imperfect restoration resulting from the implantation of hBMSCs alone.

#### LNA-Anti-miR-449a Increases Cartilage Regeneration in an OA Model

To determine whether LNA-anti-miR-449a has regenerative effects on damaged cartilage in an OA model, we induced OA surgically by destabilization of the medial meniscus (DMM) in 12-week-old rats. We induced OA for 8 weeks to establish the model, because OA was not definitively induced 6 weeks after DMM (data not shown). Eight weeks after DMM, intra-articular injections of PBS, LNA-anti-miR-sc, and LNA-anti-miR-449a were performed twice a week for up to 8 weeks (Figure 5A). In histological analysis, the LNA-anti-miR-449a-treated group showed intact surfaces resembling normal, well-differentiated chondrocytes, with reduced cartilage degradation and proteoglycan loss by safranin O and MT staining (Figure 5B). The PBS and LNA-anti-miR-sc-treated groups showed severe cartilage degradation and irregular chondrocyte morphology, severe fibrillation, and loss of proteoglycan, similar to the defect group (Figure 5B). Based on histological analysis, the LNA-anti-miR-449a-treated group had significantly lower





(legend on next page)

modified Mankin and Osteoarthritis Research Society International (OARSI) scores ( $4.00 \pm 0.88$  and  $1.88 \pm 0.83$ ; Figure 5C) compared with the other groups (20 weeks defect group:  $6.05 \pm 0.63$  and  $2.77 \pm 0.83$ ; 28 weeks defect group:  $10.22 \pm 0.69$  and  $6.22 \pm 0.50$ ; PBS group:  $10.00 \pm 0.66$  and  $5.55 \pm 0.50$ ; and LNA-anti-miR-sc group:  $10.78 \pm 1.54$  and  $5.88 \pm 0.83$ ), indicating that LNA-anti-miR-449a had a regenerative effect on damaged cartilage. We also performed IHC analysis using primary antibodies against COL2A1 and ACAN. The expression of COL2A1 and ACAN was increased on regenerated tissue in the LNA-anti-miR-449a-treated group (Figure 5D). Additionally, the expression of inflammatory marker protein cyclooxygenase-2 (COX-2) and cartilage degradation marker protein MMP-13 were significantly upregulated in surgically induced OA, PBS, and LNA-anti-miR-sc-treated groups. However, the LNA-anti-miR-449a-treated group showed a significant decrease in their expression compared with the other groups. Therefore, we confirm the inflammatory state after injection of LNA-modified miRNA (Figure S2). Together, these findings suggest that the injection of LNA-anti-miR-449a can regenerate damaged cartilage in a rat OA model.

#### LNA-Anti-miR-449a Prevents Cartilage Destruction in an OA Model

To determine whether LNA-anti-miR-449a can prevent OA progression, we induced OA by DMM in 12-week-old rats. Starting immediately after surgery, intra-articular injections of PBS, LNA-anti-miR-sc, and LNA-anti-miR-449a were performed twice a week for up to 12 weeks (Figure 6A). We performed histological analysis using safranin O and MT staining. The LNA-anti-miR-449a-treated group maintained a relatively intact cartilage structure, with well-differentiated chondrocytes surrounding the matrix, and intact proteoglycan (Figure 6B). However, nearly complete cartilage destruction, including severe fibrillation, proteoglycan loss, chondrocyte clusters, and hypertrophic chondrocytes, was observed in the defect, PBS, and LNA-anti-miR-sc-treated groups (Figure 6B). The LNA-anti-miR-449a-treated group had distinctively lower modified Mankin and OARSI scores ( $2.22 \pm 1.26$  and  $1.11 \pm 0.83$ ; Figure 6C) than the other groups (24 weeks defect group:  $8.44 \pm 0.69$  and  $4.96 \pm 0.75$ ; PBS group:  $7.88 \pm 0.83$  and  $5.66 \pm 0.33$ ; and LNA-anti-miR-sc group:  $11.67 \pm 1.76$  and  $6.74 \pm 0.35$ ). By IHC, the expression of COL2A1 and ACAN was the most abundant in the LNA-anti-miR-449a-treated group (Figure 6D). These results demonstrate that the intra-articular injection of LNA-anti-miR-449a slows down the progression of cartilage degradation in a rat OA model.

## DISCUSSION

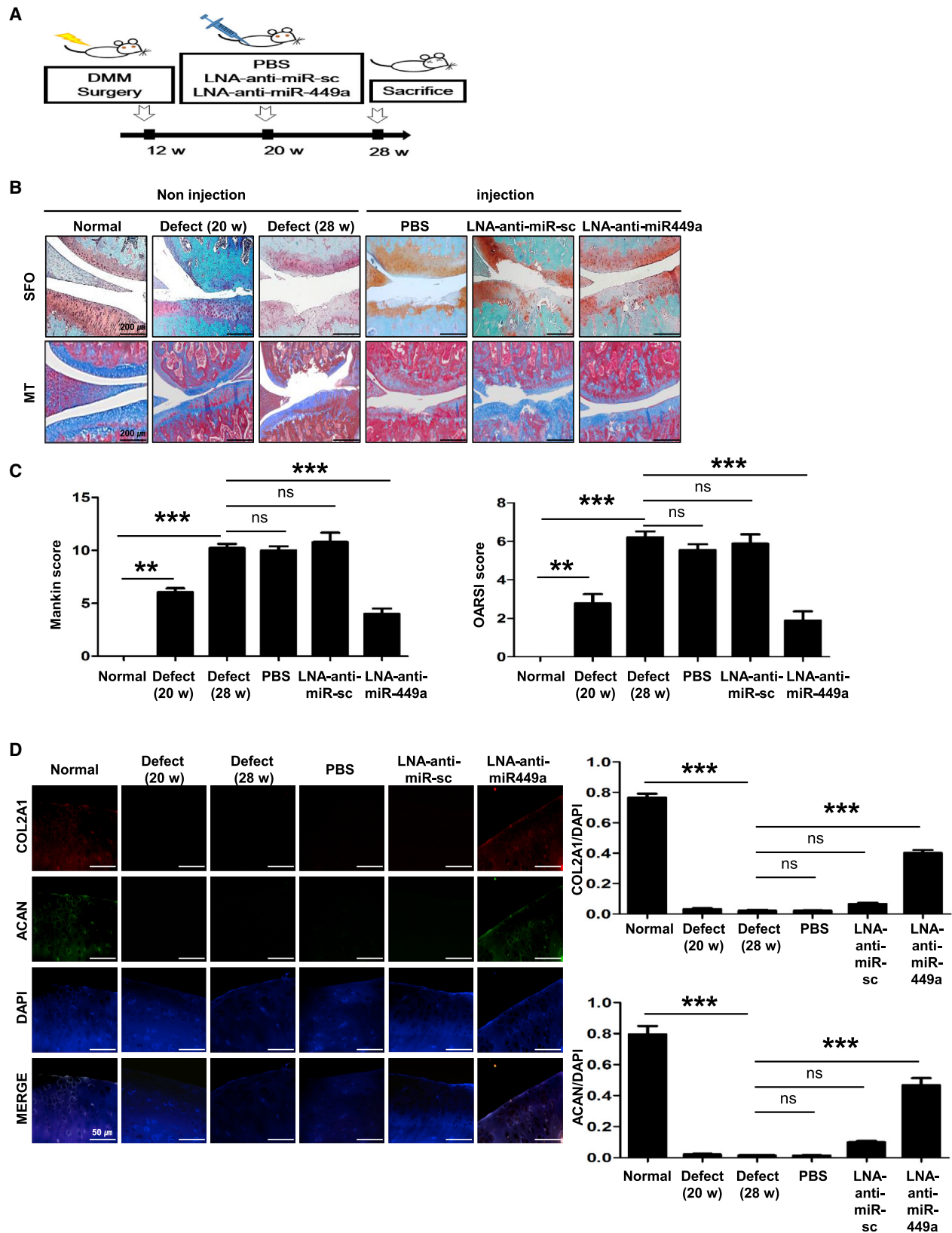
Our study is the first to report the role of anti-miR-449a *in vivo* using acute defect and OA models, and confirmed positive effect that can regenerate the damaged cartilage and slow down aggressive OA progression targeting LEF1 and SIRT1.

Previous reports have demonstrated that the intra-articular injection of hBMSCs causes no risk of immune rejection in a rat model.<sup>42,43</sup> Additionally, hBMSC treatment has been used extensively in research and clinical trials because of the stability of hBMSCs and their potential to replace damaged tissue.<sup>44,45</sup> However, studies have revealed lower regenerative capacities for hBMSCs because of the influence of culture protocols and application methods.<sup>46,47</sup> This observation is in agreement with our study, because only the hBMSCs group showed less regeneration compared with the hBMSCs with LNA-anti-miR-449a group, which had increased cartilage regeneration in the acute defect model. This may indicate synergistic effects between hBMSCs and LNA-anti-miR-449a in cartilage restoration.

Only a few studies have examined the regulation of chondrogenesis by miRNAs. They have revealed that inhibition of miR-101 prevents cartilage degeneration by targeting SOX9 in a monoiodoacetate-induced rat model of OA,<sup>48</sup> and that miR-34a regulates SIRT1 expression in human osteoarthritic chondrocytes.<sup>49</sup> Additionally, inhibition of miR-34a promotes aggressive disease progression in a rat OA model.<sup>49</sup> These groups all used adenoviral vectors for successful miRNA delivery. Viral vectors such as lentiviruses and adenoviruses have been widely used as miRNA delivery systems; however, limitations remain, including safety issues and loss of miRNA efficiency.<sup>19</sup> Poly (lactide-co-glycolide) (PLGA), a polymer, has also been widely used as an miRNA delivery system because of its low toxicity;<sup>50,51</sup> however, its use is limited by low loading efficiency.<sup>52</sup> Liposomes consisting of lipid layers have been developed for miRNA delivery;<sup>53</sup> however, these also have limitations, including toxicity and the induction of type I and type II interferons by positively charged lipids.<sup>54</sup> Therefore, more effective miRNAs delivery systems are required. In contrast, we used LNA-modified oligonucleotides to not only successfully deliver miRNAs, but also enhance miR-449a inhibition. The LNA-modified miRNA delivery system is one of the most advanced *in vivo* delivery systems. LNA can interact with complementary miRNAs with high affinity, neutralizing the targeted miRNA with no cytotoxicity.<sup>55,56</sup> We have demonstrated that LNA-anti-miR-449a is successfully delivered to defect sites, where it serves dual positive roles, regenerating damaged cartilage and preventing OA

#### Figure 4. Increased Cartilage Regeneration by LNA-Anti-miR-449a in an Acute Defect Model

(A) Experimental design for cartilage regeneration induced by acute osteochondral defects. (B) Gross morphology of osteochondral defects after 4 weeks. (C) Histological analysis of osteochondral defects observed using H&E and MT staining. Scale bars, 500  $\mu$ m (original magnification  $\times 4$ ). (D) Histological analysis of osteochondral defects observed using safranin O staining. Scale bars, 500  $\mu$ m (original magnification  $\times 4$ ) and 100  $\mu$ m (original magnification  $\times 20$ ). (E) Quantification of safranin O staining. (F) Quantification of histology by O'Driscoll score based on safranin O staining. (G) Left: IHC analysis of COL2A1 (PE; red fluorescence) and ACAN (FITC; green fluorescence) in an acute defect model. Scale bar, 50  $\mu$ m (original magnification  $\times 40$ ). Right: quantification of IHC analysis. Data are defined as mean  $\pm$  SD. p values were calculated compared with the defect group: \*p < 0.05; \*\*\*p < 0.001 (n = 7 for each group).



(legend on next page)

progression by targeting LEF1 and SIRT1. Hence, our results provide insights on the utility of LNAs as *in vivo* miRNA delivery systems.

In a previous report, we showed that miR-449a negatively regulates LEF1 expression during hBMSC chondrogenesis.<sup>33</sup> This result suggested that the inhibition of miR-449a would promote the chondrogenic differentiation of hBMSCs by increasing LEF1 expression. Here, our *in vivo* study confirmed that miR-449a inhibition causes the regeneration of damaged cartilage in an acute defect model and OA model.

SIRT1 plays an inhibitory role in IL-1 $\beta$ -induced cartilage destruction associated with OA.<sup>57,58</sup> In a previous report, we showed that miR-449a regulates the expression of SIRT1, which has anti-inflammatory effects on OA chondrocytes.<sup>34</sup> We confirmed that the inhibition of miR-449a has a protective effect, inhibiting the expression of catabolic genes and restoring the expression of anabolic genes by targeting SIRT1 during IL-1 $\beta$ -induced cartilage degradation. Combined with these previous results, the *in vivo* results in this study suggest that miR-449a may be a promising novel therapeutic target for the prevention of cartilage degeneration.

Overall, our observations strongly indicate dual positive effects of silencing miR-449a, regenerating damaged cartilage and preventing OA progression by targeting LEF1 and SIRT1. These results suggest that miR-449a could be a promising therapeutic target for OA and other cartilage degenerative disorders.

## MATERIALS AND METHODS

### Culture of hBMSCs

Bone marrow aspirates were obtained from the posterior iliac crests of 10 healthy adult donors with a mean age of 47.5 years (range: 31–65 years), with approval from the Institutional Review Board of Yonsei University College of Medicine (IRB No. 4-2017-0232), and all participants agreed to participation. Cells were cultured and selected by adherence on a plastic culture plate surface, and their validations were confirmed by flow cytometry as in a previous study,<sup>59</sup> then cultured for 7 days in DMEM-low glucose (GIBCO, USA) with 10% fetal bovine serum (FBS; GIBCO, USA) and 1% antibiotic-antimycotic solution (GIBCO, USA). Cells were subcultured for up to three passages, and all experiments were carried out in triplicate.

### Chondrogenic Differentiation of hBMSCs

DMEM-high glucose (DMEM-HG; GIBCO, USA) with 1 $\times$  antibiotic-antimycotic solution, 1 $\times$  insulin transferrin selenium-A (ITS; Invitrogen, Carlsbad, CA, USA), 50  $\mu$ g/mL ascorbic acid (Sigma, St. Louis, MO, USA), and 10 ng/mL transforming growth factor (TGF)- $\beta$ 3 (R&D Systems; Minneapolis, MN, USA) was used for the

chondrogenic differentiation of hBMSCs. For micromass culture,  $1 \times 10^5$  hBMSCs were dropped in the center of each well of a 24-well plate. After 2 hr, chondrogenic medium was added. The medium was replaced every 3 days.

### Cytotoxicity Assay

A cytotoxicity assay was performed using the MTT assay in 48-well plates. EZ-Cytox cell viability reagents (Daeil Lab, Seoul, Korea) and 300  $\mu$ L of fresh medium were added, and the samples were incubated at 37°C for 4 hr. The absorbance was measured at 540 nm.

### Transfection of miRNA

Cells were transfected with miR-scramble control (miR-sc; Genolution, Seoul, Korea), miR-449a mimic (Genolution, Seoul, Korea), anti-miR-sc mimic (ST Pharm, Seoul, Korea), and anti-miR-449a mimic (ST Pharm, Seoul, Korea) at 100 nM using Lipofectamine LTX & Plus Reagent (Invitrogen, Carlsbad, CA, USA) according to the manufacturer's instructions. LNA-modified oligonucleotides were used as a delivery system into cartilage joints, and LNA was synthesized as unconjugated and fully phosphorothiolated oligonucleotides (Exiqon, Vedbaek, Denmark). LNA-anti-miR-sc and LNA-anti-miR-449a were directly applied to hBMSCs. After 48 hr, cells were harvested, and chondrogenic differentiation was induced by micromass culture. A list of all miRNA sequences used is provided in Table S1.

### Real-Time qPCR

Total RNA was extracted from harvested cells using TRIzol Reagent (Invitrogen, Carlsbad, CA, USA), and cDNA was synthesized for real-time qPCR (Applied Biosystems, Foster City, CA, USA). miR-specific real-time qPCR was performed according to guidelines of a manufacturer, and U6 small nuclear RNA (snRNA) was used as a control to quantify miRNAs (Clontech, Palo Alto, CA, USA). A list of all primer sequences used is provided in Table S2.

### Western Blot Analysis

For protein extraction, cells were harvested and lysed in lysis buffer (50 mM Tris [pH 7.4], 150 mM NaCl, 1% tergitol-type NP-40 [NP-40], and 0.1% SDS) and processed as previously described.<sup>34</sup> The primary antibodies used targeted LEF1, SIRT1, SOX9, and GAPDH (all from Santa Cruz Biotechnology, USA).

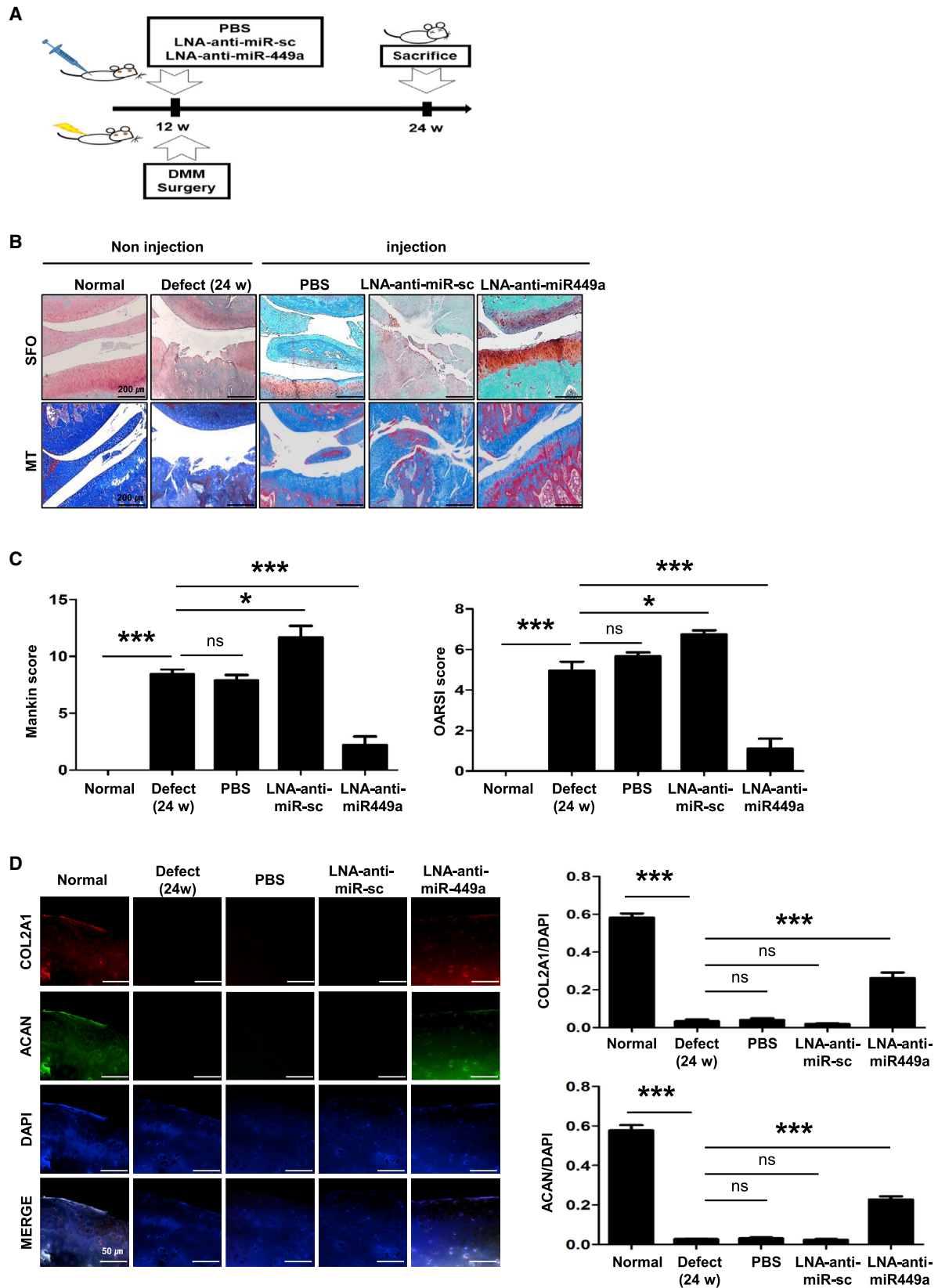
### *In Vivo* Surgical Induction of an Acute Defect Model in Rats

The Committee on the Ethics of Animal Experiments of Yonsei University College of Medicine approved all animal experiments and protocols (permit no. 2015-0168). Male Sprague-Dawley rats ( $n = 7$  per group) at 12 weeks of age were anaesthetized with an intra-peritoneal

## Figure 5. Increased Cartilage Regeneration by LNA-Anti-miR-449a in an OA Model

(A) Experimental design for cartilage regeneration induced by DMM. (B) Representative safranin O staining and MT staining of histological sections of articular cartilage. Scale bar, 200  $\mu$ m (original magnification  $\times 10$ ). (C) Histological evaluation by modified Mankin and OARS scoring systems (left and right panels, respectively). (D) Left: COL2A1 and ACAN expression on the regenerated cartilage surface by IHC analysis, with DAPI counterstaining. Scale bar, 50  $\mu$ m (original magnification  $\times 40$ ). Right: quantification of IHC analysis. Data are defined as mean  $\pm$  SD. p values were calculated compared with the defect group. \*\*p < 0.01; \*\*\*p < 0.001 ( $n = 7$  for each group).





(legend on next page)

injection of Zoletil (30 mg/kg) and Rompun (10 mg/kg). To expose the rat knee joint, we made a para-patellar incision using a surgical blade. After lateral dislocation of the patella, we created an osteochondral defect (2.0 mm in diameter and 1.5 mm in depth) on the patellar groove of the distal femur using a trephine burr. Next, scaffolds were inserted into the osteochondral defect sites, and we randomly allocated the animals into four groups as follows: (1) untreated defect, (2) hBMSCs only, (3) hBMSCs with LNA-anti-miR-sc, and (4) hBMSCs with LNA-anti-miR-449a. Fibrin gel (Greenplast Kit; Green Cross, Seoul, Korea) was used as a scaffold according to the manufacturer's instructions. Finally, the incision site was closed with Vicryl, and Metacam (1 mg/kg) was used as an analgesic. Rats were sacrificed 4 and 8 weeks after surgery, and the knee joints were harvested.

#### **In Vivo DMM in Rats and Intra-articular Injection of LNA-Anti-miR-449a**

To establish a rat model of OA, we prepared the right knees of 12-week-old male Sprague-Dawley rats ( $n = 7$  per group) for DMM surgery according to a previous study.<sup>60</sup> In brief, the medial meniscus (MM) and medial meniscotibial ligament (MMTL) were opened following the dissection of the fat pad. Then, the menisci were devitalized due to transection of the MMTL with no. 11 blade, and the wound was closed with 3-0 Vicryl.<sup>60</sup> Animals were randomly allocated into four groups as follows: DMM without treatment (defect), DMM with PBS, DMM with LNA-anti-miR-sc, and DMM with LNA-anti-miR-449a. Intra-articular injections of 50  $\mu$ L of PBS, LNA-anti-miR-sc (100 nM), and LNA-anti-miR-449a (100 nM) were performed 8 weeks after DMM surgery twice a week and immediately following DMM surgery twice a week for 12 weeks.<sup>55,61</sup> At 8, 12, and 16 weeks post-DMM, the rats were sacrificed under anesthesia and knee joints were harvested.

#### **Histological and IHC Analysis**

Knee joints were fixed with 3.7% formaldehyde, decalcified with Calci-Clear Rapid (National Diagnostics, Atlanta, GA, USA), embedded in paraffin, and cut into 100- $\mu$ m sections. For histological analysis, the sections were deparaffinized in xylene and serially rehydrated in ethanol. The sections were sequentially stained with MT, H&E, Alcian blue and safranin O staining according to conventional protocols. To evaluate the histological assessment of the acute defect model, we used the O'Driscoll scoring system<sup>62</sup> and as demonstrated in Table S3; to evaluate the histological assessment of the OA models, we used modified Mankin and OARSI score systems for cartilage regeneration following as demonstrated in Table S4.<sup>63,64</sup> For IHC, primary antibodies against ACAN, COL2A1, MMP13 (all from Santa Cruz Biotechnology, USA), and COX2 (BD Biosciences, USA) were used. All histological results were evaluated fairly by independent

blind assessment. The numbers of positively stained cells were calculated using ImageJ 1.51f software (NIH).

#### **Statistical Analysis**

For each experiment, samples were analyzed in triplicate. For comparisons of over three groups, we used one-way ANOVA and post hoc comparison with the Tukey correction. Two-tailed independent *t* tests were used for comparisons between two groups. GraphPad Prism software (version 6.0) was used for statistical analysis. *p* values less than 0.05 were considered statistically significant. All data are presented as mean  $\pm$  SD.

#### **SUPPLEMENTAL INFORMATION**

Supplemental Information includes two figures, four tables, and Supplemental Materials and Methods and can be found with this article online at <https://doi.org/10.1016/j.omtn.2018.09.015>.

#### **AUTHOR CONTRIBUTIONS**

D.B. wrote the manuscript. D.B. and K.W.P. performed all *in vitro* and *in vivo* experiments together. K.-M.L. discussed the data. J.W.S. devised the animal surgery protocols and suggested methodology for the animal studies. S.M.C. performed the *in vivo* experiments. K.H.P. analyzed the data and kindly recommended experiments. J.W.L. and S.-H.K. supervised the preparation of this manuscript and provided important intellectual contributions to the final draft.

#### **CONFLICTS OF INTEREST**

There authors have no conflicts of interest.

#### **ACKNOWLEDGMENTS**

This work was supported by grants from the Ministry of Science of Republic of Korea (grant NRF-2014R1A1A1007983) and by the Mid-career Researcher Program through an NRF grant funded by the MEST (NRF-2018R1A2B6007376).

#### **REFERENCES**

- Zhang, W., Ouyang, H., Dass, C.R., and Xu, J. (2016). Current research on pharmacologic and regenerative therapies for osteoarthritis. *Bone Res.* 4, 15040.
- Yoon, D.S., Lee, K.M., Kim, S.H., Kim, S.H., Jung, Y., Kim, S.H., Park, K.H., Choi, Y., Ryu, H.A., Choi, W.J., and Lee, J.W. (2016). Synergistic action of IL-8 and bone marrow concentrate on cartilage regeneration through upregulation of chondrogenic transcription factors. *Tissue Eng. Part A* 22, 363–374.
- Mobasheri, A., Kalamegam, G., Musumeci, G., and Batt, M.E. (2014). Chondrocyte and mesenchymal stem cell-based therapies for cartilage repair in osteoarthritis and related orthopaedic conditions. *Maturitas* 78, 188–198.
- Richardson, S.M., Kalamegam, G., Pushparaj, P.N., Matta, C., Memic, A., Khademhosseini, A., Mobasheri, R., Poletti, F.L., Hoyland, J.A., and Mobasheri, A. (2016). Mesenchymal stem cells in regenerative medicine: focus on articular cartilage and intervertebral disc regeneration. *Methods* 99, 69–80.

#### **Figure 6. Prevention of Cartilage Destruction by LNA-Anti-miR-449a in an OA Model**

(A) Experimental design for prevention of cartilage degeneration induced by DMM. (B) Representative safranin O and MT staining of histological sections of articular cartilage 12 weeks after DMM surgery. Scale bar, 200  $\mu$ m (original magnification  $\times 10$ ). (C) Histological evaluation by modified Mankin and OARSI scoring systems (left and right panels, respectively). (D) Left: COL2A1 and ACAN expression on the regenerated cartilage surface by IHC analysis, with DAPI counterstaining. Scale bar, 50  $\mu$ m (original magnification  $\times 40$ ). Right: quantification of IHC analysis. Data are defined as mean  $\pm$  SD. *p* values were calculated compared with the defect group. \**p* < 0.05; \*\*\**p* < 0.001 ( $n = 7$  for each group).

5. Nombela-Arrieta, C., Ritz, J., and Silberstein, L.E. (2011). The elusive nature and function of mesenchymal stem cells. *Nat. Rev. Mol. Cell Biol.* 12, 126–131.
6. Barry, F., and Murphy, M. (2013). Mesenchymal stem cells in joint disease and repair. *Nat. Rev. Rheumatol.* 9, 584–594.
7. Mahmoudifar, N., and Doran, P.M. (2012). Chondrogenesis and cartilage tissue engineering: the longer road to technology development. *Trends Biotechnol.* 30, 166–176.
8. Chen, F.H., and Tuan, R.S. (2008). Mesenchymal stem cells in arthritic diseases. *Arthritis Res. Ther.* 10, 223.
9. Wang, M., Yuan, Z., Ma, N., Hao, C., Guo, W., Zou, G., Zhang, Y., Chen, M., Gao, S., Peng, J., et al. (2017). Advances and prospects in stem cells for cartilage regeneration. *Stem Cells Int.* 2017, 4130607.
10. van Buul, G.M., Villafuertes, E., Bos, P.K., Waarsing, J.H., Kops, N., Narcisi, R., Weinans, H., Verhaar, J.A., Bernsen, M.R., and van Osch, G.J. (2012). Mesenchymal stem cells secrete factors that inhibit inflammatory processes in short-term osteoarthritic synovium and cartilage explant culture. *Osteoarthritis Cartilage* 20, 1186–1196.
11. Nejadnik, H., Diecke, S., Lenkov, O.D., Chapelin, F., Donig, J., Tong, X., Derugin, N., Chan, R.C., Gaur, A., Yang, F., et al. (2015). Improved approach for chondrogenic differentiation of human induced pluripotent stem cells. *Stem Cell Rev.* 11, 242–253.
12. Wei, Y., Zeng, W., Wan, R., Wang, J., Zhou, Q., Qiu, S., and Singh, S.R. (2012). Chondrogenic differentiation of induced pluripotent stem cells from osteoarthritic chondrocytes in alginate matrix. *Eur. Cell. Mater.* 23, 1–12.
13. Shi, Y., Inoue, H., Wu, J.C., and Yamanaka, S. (2017). Induced pluripotent stem cell technology: a decade of progress. *Nat. Rev. Drug Discov.* 16, 115–130.
14. Steinert, A.F., Nöth, U., and Tuan, R.S. (2008). Concepts in gene therapy for cartilage repair. *Injury* 39 (Suppl 1), S97–S113.
15. Burke, J., Hunter, M., Kolhe, R., Isaacs, C., Hamrick, M., and Fulzele, S. (2016). Therapeutic potential of mesenchymal stem cell based therapy for osteoarthritis. *Clin. Transl. Med.* 5, 27.
16. Trippel, S.B., Ghivizzani, S.C., and Nixon, A.J. (2004). Gene-based approaches for the repair of articular cartilage. *Gene Ther.* 11, 351–359.
17. Ha, M., and Kim, V.N. (2014). Regulation of microRNA biogenesis. *Nat. Rev. Mol. Cell Biol.* 15, 509–524.
18. He, L., and Hannon, G.J. (2004). MicroRNAs: small RNAs with a big role in gene regulation. *Nat. Rev. Genet.* 5, 522–531.
19. van Rooij, E., and Kauppinen, S. (2014). Development of microRNA therapeutics is coming of age. *EMBO Mol. Med.* 6, 851–864.
20. Li, Z., and Rana, T.M. (2014). Therapeutic targeting of microRNAs: current status and future challenges. *Nat. Rev. Drug Discov.* 13, 622–638.
21. Rupaimoole, R., and Slack, F.J. (2017). MicroRNA therapeutics: towards a new era for the management of cancer and other diseases. *Nat. Rev. Drug Discov.* 16, 203–222.
22. Rupaimoole, R., Calin, G.A., Lopez-Berestein, G., and Sood, A.K. (2016). miRNA deregulation in cancer cells and the tumor microenvironment. *Cancer Discov.* 6, 235–246.
23. Broderick, J.A., and Zamore, P.D. (2011). MicroRNA therapeutics. *Gene Ther.* 18, 1104–1110.
24. Garzon, R., Marcucci, G., and Croce, C.M. (2010). Targeting microRNAs in cancer: rationale, strategies and challenges. *Nat. Rev. Drug Discov.* 9, 775–789.
25. Mirzamohammadi, F., Papaioannou, G., and Kobayashi, T. (2014). MicroRNAs in cartilage development, homeostasis, and disease. *Curr. Osteoporos. Rep.* 12, 410–419.
26. Asahara, H. (2016). Current status and strategy of microRNA research for cartilage development and osteoarthritis pathogenesis. *J. Bone Metab.* 23, 121–127.
27. Yuan, Y., Zhang, G.Q., Chai, W., Ni, M., Xu, C., and Chen, J.Y. (2016). Silencing of microRNA-138-5p promotes IL-1 $\beta$ -induced cartilage degradation in human chondrocytes by targeting FOXO1: miR-138 promotes cartilage degradation. *Bone Joint Res.* 5, 523–530.
28. Mao, G., Zhang, Z., Huang, Z., Chen, W., Huang, G., Meng, F., Zhang, Z., and Kang, Y. (2017). MicroRNA-92a-3p regulates the expression of cartilage-specific genes by directly targeting histone deacetylase 2 in chondrogenesis and degradation. *Osteoarthritis Cartilage* 25, 521–532.
29. Karlsen, T.A., de Souza, G.A., Ødegaard, B., Engebretsen, L., and Brinchmann, J.E. (2016). microRNA-140 inhibits inflammation and stimulates chondrogenesis in a model of interleukin 1 $\beta$ -induced osteoarthritis. *Mol. Ther. Nucleic Acids* 5, e373.
30. Miyaki, S., Sato, T., Inoue, A., Otsuki, S., Ito, Y., Yokoyama, S., Kato, Y., Takemoto, F., Nakasa, T., Yamashita, S., et al. (2010). MicroRNA-140 plays dual roles in both cartilage development and homeostasis. *Genes Dev.* 24, 1173–1185.
31. Lolli, A., Narcisi, R., Lambertini, E., Penolazzi, L., Angelozzi, M., Kops, N., Gasparini, S., van Osch, G.J., and Piva, R. (2016). Silencing of antichondrogenic microRNA-221 in human mesenchymal stem cells promotes cartilage repair in vivo. *Stem Cells* 34, 1801–1811.
32. Wang, H., Zhang, H., Sun, Q., Wang, Y., Yang, J., Yang, J., Zhang, T., Luo, S., Wang, L., Jiang, Y., et al. (2017). Intra-articular delivery of antago-miR-483-5p inhibits osteoarthritis by modulating Matrilin 3 and tissue inhibitor of metalloproteinase 2. *Mol. Ther.* 25, 715–727.
33. Paik, S., Jung, H.S., Lee, S., Yoon, D.S., Park, M.S., and Lee, J.W. (2012). miR-449a regulates the chondrogenesis of human mesenchymal stem cells through direct targeting of lymphoid enhancer-binding factor-1. *Stem Cells Dev.* 21, 3298–3308.
34. Park, K.W., Lee, K.M., Yoon, D.S., Park, K.H., Choi, W.J., Lee, J.W., and Kim, S.H. (2016). Inhibition of microRNA-449a prevents IL-1 $\beta$ -induced cartilage destruction via SIRT1. *Osteoarthritis Cartilage* 24, 2153–2161.
35. Buhrmann, C., Busch, F., Shayan, P., and Shakibaei, M. (2014). Sirtuin-1 (SIRT1) is required for promoting chondrogenic differentiation of mesenchymal stem cells. *J. Biol. Chem.* 289, 22048–22062.
36. Kurreck, J., Wyszko, E., Gillen, C., and Erdmann, V.A. (2002). Design of antisense oligonucleotides stabilized by locked nucleic acids. *Nucleic Acids Res.* 30, 1911–1918.
37. Nedaieina, R., Sharifi, M., Avan, A., Kazemi, M., Rafiee, L., Ghayour-Mobarhan, M., and Salehi, R. (2016). Locked nucleic acid anti-miR-21 inhibits cell growth and invasive behaviors of a colorectal adenocarcinoma cell line: LNA-anti-miR as a novel approach. *Cancer Gene Ther.* 23, 246–253.
38. Thakral, S., and Ghoshal, K. (2015). miR-122 is a unique molecule with great potential in diagnosis, prognosis of liver disease, and therapy both as miRNA mimic and antimir. *Curr. Gene Ther.* 15, 142–150.
39. Zhang, Y., Roccaro, A.M., Rombaoa, C., Flores, L., Obad, S., Fernandes, S.M., Sacco, A., Liu, Y., Ngo, H., Quang, P., et al. (2012). LNA-mediated anti-miR-155 silencing in low-grade B-cell lymphomas. *Blood* 120, 1678–1686.
40. Obad, S., dos Santos, C.O., Petri, A., Heidenblad, M., Broom, O., Ruse, C., Fu, C., Lindow, M., Stenvang, J., Straarup, E.M., et al. (2011). Silencing of microRNA families by seed-targeting tiny LNAs. *Nat. Genet.* 43, 371–378.
41. Murphy, B.L., Obad, S., Bihannic, L., Ayrault, O., Zindy, F., Kauppinen, S., and Roussel, M.F. (2013). Silencing of the miR-17–92 cluster family inhibits medulloblastoma progression. *Cancer Res.* 73, 7068–7078.
42. Horie, M., Choi, H., Lee, R.H., Reger, R.L., Ylostalo, J., Muneta, T., Sekiya, I., and Prockop, D.J. (2012). Intra-articular injection of human mesenchymal stem cells (MSCs) promote rat meniscal regeneration by being activated to express Indian hedgehog that enhances expression of type II collagen. *Osteoarthritis Cartilage* 20, 1197–1207.
43. Chung, J.Y., Song, M., Ha, C.W., Kim, J.A., Lee, C.H., and Park, Y.B. (2014). Comparison of articular cartilage repair with different hydrogel-human umbilical cord blood-derived mesenchymal stem cell composites in a rat model. *Stem Cell Res. Ther.* 5, 39.
44. Wang, Y., Han, Z.B., Song, Y.P., and Han, Z.C. (2012). Safety of mesenchymal stem cells for clinical application. *Stem Cells Int.* 2012, 652034.
45. Wyles, C.C., Houdek, M.T., Behfar, A., and Sierra, R.J. (2015). Mesenchymal stem cell therapy for osteoarthritis: current perspectives. *Stem Cells Cloning* 8, 117–124.
46. Mahmud, N., Pang, W., Cobbs, C., Alur, P., Borneman, J., Dodds, R., Archambault, M., Devine, S., Turian, J., Bartholomew, A., et al. (2004). Studies of the route of administration and role of conditioning with radiation on unrelated allogeneic mismatched mesenchymal stem cell engraftment in a nonhuman primate model. *Exp. Hematol.* 32, 494–501.
47. Nasef, A., Fouillard, L., El-Taguri, A., and Lopez, M. (2007). Human bone marrow-derived mesenchymal stem cells. *Libyan J. Med.* 2, 190–201.

48. Dai, L., Zhang, X., Hu, X., Zhou, C., and Ao, Y. (2012). Silencing of microRNA-101 prevents IL-1 $\beta$ -induced extracellular matrix degradation in chondrocytes. *Arthritis Res. Ther.* 14, R268.
49. Yan, S., Wang, M., Zhao, J., Zhang, H., Zhou, C., Jin, L., Zhang, Y., Qiu, X., Ma, B., and Fan, Q. (2016). MicroRNA-34a affects chondrocyte apoptosis and proliferation by targeting the SIRT1/p53 signaling pathway during the pathogenesis of osteoarthritis. *Int. J. Mol. Med.* 38, 201–209.
50. Kulkarni, R.K., Moore, E.G., Hegyeli, A.F., and Leonard, F. (1971). Biodegradable poly(lactic acid) polymers. *J. Biomed. Mater. Res.* 5, 169–181.
51. Blum, J.S., and Saltzman, W.M. (2008). High loading efficiency and tunable release of plasmid DNA encapsulated in submicron particles fabricated from PLGA conjugated with poly-L-lysine. *J. Control. Release* 129, 66–72.
52. Yang, X.Z., Dou, S., Sun, T.M., Mao, C.Q., Wang, H.X., and Wang, J. (2011). Systemic delivery of siRNA with cationic lipid assisted PEG-PLA nanoparticles for cancer therapy. *J. Control. Release* 156, 203–211.
53. Morrissey, D.V., Lockridge, J.A., Shaw, L., Blanchard, K., Jensen, K., Breen, W., Hartsough, K., Machemer, L., Radka, S., Jadhav, V., et al. (2005). Potent and persistent in vivo anti-HBV activity of chemically modified siRNAs. *Nat. Biotechnol.* 23, 1002–1007.
54. Pecot, C.V., Calin, G.A., Coleman, R.L., Lopez-Berestein, G., and Sood, A.K. (2011). RNA interference in the clinic: challenges and future directions. *Nat. Rev. Cancer* 11, 59–67.
55. Elmén, J., Lindow, M., Schütz, S., Lawrence, M., Petri, A., Obad, S., Lindholm, M., Hedtjärn, M., Hansen, H.F., Berger, U., et al. (2008). LNA-mediated microRNA silencing in non-human primates. *Nature* 452, 896–899.
56. Elmén, J., Lindow, M., Silahtaroglu, A., Bak, M., Christensen, M., Lind-Thomsen, A., Hedtjärn, M., Hansen, J.B., Hansen, H.F., Straarup, E.M., et al. (2008). Antagonism of microRNA-122 in mice by systemically administered LNA-antimiR leads to up-regulation of a large set of predicted target mRNAs in the liver. *Nucleic Acids Res.* 36, 1153–1162.
57. Matsuzaki, T., Matsushita, T., Takayama, K., Matsumoto, T., Nishida, K., Kuroda, R., and Kurosaka, M. (2014). Disruption of Sirt1 in chondrocytes causes accelerated progression of osteoarthritis under mechanical stress and during ageing in mice. *Ann. Rheum. Dis.* 73, 1397–1404.
58. Liu-Bryan, R., and Terkeltaub, R. (2015). Emerging regulators of the inflammatory process in osteoarthritis. *Nat. Rev. Rheumatol.* 11, 35–44.
59. Lee, S., Yoon, D.S., Paik, S., Lee, K.M., Jang, Y., and Lee, J.W. (2014). microRNA-495 inhibits chondrogenic differentiation in human mesenchymal stem cells by targeting Sox9. *Stem Cells Dev.* 23, 1798–1808.
60. Glasson, S.S., Blanchet, T.J., and Morris, E.A. (2007). The surgical destabilization of the medial meniscus (DMM) model of osteoarthritis in the 129/SvEv mouse. *Osteoarthritis Cartilage* 15, 1061–1069.
61. Takayama, K., Kawakami, Y., Kobayashi, M., Greco, N., Cummins, J.H., Matsushita, T., Kuroda, R., Kurosaka, M., Fu, F.H., and Huard, J. (2014). Local intra-articular injection of rapamycin delays articular cartilage degeneration in a murine model of osteoarthritis. *Arthritis Res. Ther.* 16, 482.
62. O'Driscoll, S.W., Keeley, F.W., and Salter, R.B. (1988). Durability of regenerated articular cartilage produced by free autogenous periosteal grafts in major full-thickness defects in joint surfaces under the influence of continuous passive motion. A follow-up report at one year. *J. Bone Joint Surg. Am.* 70, 595–606.
63. van der Sluijs, J.A., Geesink, R.G.T., van der Linden, A.J., Bulstra, S.K., Kuyper, R., and Drukker, J. (1992). The reliability of the Mankin score for osteoarthritis. *J. Orthop. Res.* 10, 58–61.
64. Gerwin, N., Bendele, A.M., Glasson, S., and Carlson, C.S. (2010). The OARSI histopathology initiative - recommendations for histological assessments of osteoarthritis in the rat. *Osteoarthritis Cartilage* 18 (Suppl 3), S24–S34.